Kinetics and Properties of a Photopolymerized Dimethacrylate Oligomer

WAYNE D. COOK

Medical Devices and Dental Products Branch, Department of Community Services and Health, 240 Langridge Street, Abbotsford, Victoria, Australia 3067

SYNOPSIS

The free radical photopolymerization of two urethane dimethacrylate oligomer systems, used in dentistry as elastomeric impression materials, was investigated. When cured in thick section, these materials have a limited depth of cure that depends on the irradiation conditions. A mathematical model is presented that considers the spatial dependence of the polymerization process on the attenuated radiation intensity and the local concentration of radical scavenging inhibitors. The predicted dependence of the depth of cure on the logarithm of radiation intensity and exposure time is confirmed. DSC studies revealed that for thin sections the rate of polymerization had the conventional square root dependence on radiation intensity over a 1000-fold range of intensities. These results are discussed in terms of a decoupling of the mobility of the pendant methacrylate group from the chain to which it is attached. In an oxygen environment, inhibition of the photopolymerization caused an induction period that was proportional to the reciprocal radiation intensity. Modulus measurements during cure also illustrated the rapid nature of photopolymerization process and showed that in comparison to conventional two-component materials used for the same purpose the rates of buildup in properties for the photocured materials were superior. The tear energy of the cured photocured materials were compared with conventional types of elastomeric impression material, and the differences were interpreted in terms of energy dissipation mechanisms.

INTRODUCTION

The use of radiation as the initiating step in polymerization has become increasingly common in the last two decades.[1,2] Applications range from photolithography[2] and a range of electronic applications[1] to the technique of stereolithography[3] used to photocure complex three-dimensional shapes. For many applications utilizing free-radical polymerization, the monomer system is used as a thin film so that oxygen inhibition may be critical. In other cases, the attenuation of the radiation by the resin system may be another limitation. For these reasons, more attention is being directed at photopolymerization in nonideal circumstances where inhibition and depth effects are found.

Since the 1960s, the technique of photopolymerization has found increasing application in the dental field. The first materials, used for restoring dental caries, were based on dimethacrylates that were intitiated[4] by the UV-photolysis of benzoin alkyl ethers. Because of the potential ocular hazard and limited intensity of the UV sources, they have been superseded by visible light curing systems. The photochemical basis of the visible light curing system is invariably camphor-quinone, which on exposure to 450—500 nm radiation (the absorption maximum of camphor-quinone is 470 nm Ref. 4) is believed to undergo charge transfer with an amine coinitiator to yield the initiating radicals.[5] This photocuring principle has also been applied to the fabrication of dentures from dimethyacrylate resins. Most recently, a photocuring system has been developed for taking an accurate, elastomeric impression of the teeth and oral mucosal surfaces. In each of the above three applications, the attenuation of the radiation in the material and the inhibition of the polymerization by oxygen cannot be ignored.

This paper reports on the photopolymerization

Journal of Applied Polymer Science, Vol. 42, 2209–2222 (1991)
 CCC 0021-8995/91/082209-14$04.00

behavior and properties of a commercial dimethacrylate system that is used to form elastomeric impressions of the oral tissues.

EXPERIMENTAL

The resin system was supplied as a fluid and a viscous paste by the manufacturer, Dentsply International Inc. (Milford, DE), under the trade names of Genesis Light Body (denoted here as GNLB) and Genesis Heavy Body (GNHB), respectively. Samples were photocured by a Visilux-2 dental photopolymerization source (3M, St. Paul, MN, USA) which consists of a 75 W tungsten/halogen lamp, a series of optical lenses, and filters and a fused fiber optic light-guide with a 7 mm exit window. This source emits continuous band radiation predominantly in the region 450–500 nm and has a maximum spectral radiance emittance of 7.8×10^{-3} W/cm^2/nm at 470 nm—the spectral distribution of this source has been published elsewhere.[6] The intensity of the lamp was found to vary with time during operation, decreasing by 7% in the first 10 s and by another 9% during the following 10 min. For studies of the influence of radiation intensity on the polymerization process, glass neutral density filters with transmissions ranging from 50 to 0.001% were used. Because the effect of the instability of the light source during operation was small compared with the overall range of intensities employed, it was neglected.

Table I lists some analytical data for the materials. The filler level was determined by $CHCl_3$ extraction of the organic components from the pastes and the wt % of the plasticizer was measured after a 24 h soxhlet extraction of "fully cured" samples of the materials with $CHCl_3$. Preliminary studies revealed that the photocurable materials could not be polymerized by radiation having wavelengths above 500 nm, which is consistent with the use of camphor-quinone (λ_{max} = 470 nm) as the photoinitiator. The concentration of the camphor-quinone was determined by gas chromatography[7] (see Table I).

Infrared spectroscopy was performed with a model 683 Perkin-Elmer instrument utilizing an analog-to-digital converter. The presence of ester groups (1720 cm^{-1}), etheric linkages (1100 cm^{-1}), amide NH stretch (3350 cm^{-1}), amide NH bend (1525 cm^{-1}), and C=C stretch (1640 cm^{-1}) in the IR spectrum (Fig. 1) of the uncured paste extract is consistent with the manufacturer's claim that the materials are based on a polyether-backbone urethane dimethacrylate. Absorbances at 1370 and 2940 cm^{-1} suggest that the backbone is polypropylene oxide. The presence of ester (1720 cm^{-1}) and aromatic (1605 cm^{-1}) bands in the IR spectrum of the extract of the cured material (Fig. 1) indicates a phthalate-like plasticizer. The IR spectrum of the extracted gel is similar to the uncured material with the exception of the aromatic peak (which is contained in the plasticizer) and the olefinic peak.

By use of a multiple internal reflectance (MIR) accessory, the variation of the degree of conversion of the methacrylate groups with time was monitored by comparison of the methacrylate band at 1640 cm^{-1} relative the aromatic band at 1605 cm^{-1}. Samples of the material were spread over the width of the MIR TlBrI crystal, and a glass slide was placed over the material to exclude air. After uniform irradiation of the material with the photocuring source, greater than 95% conversion of the methacrylate unsaturation was observed.

Assuming that the molar absorption coefficient for the methacrylate group in the dimethacrylate oligomers is equal to that for triethylene glycol dimethacrylate (TEGDMA), the concentration of methacrylate groups in GNLB and GNHB (see Table I) were determined by the standard addition method. This was performed by comparison of the absorbance ratio of the 1640 cm^{-1} methacrylate band to the reference 1605 cm^{-1} (aromatic) peak in pastes containing various amounts of TEGDMA.

Proton NMR spectra of the extracts were ob-

Table I Composition of the Photocured Materials

	GNLB	GNHB
Wt % dimethacrylate	40.2	37.4
Concentration of methacrylate groups (mmol/g of paste)	0.48 ± 0.15	0.39 ± 0.05
Wt % plasticizer	19.4	12.6
Wt % filler	40.4	50.0
Wt % camphor-quinone	0.124	0.076

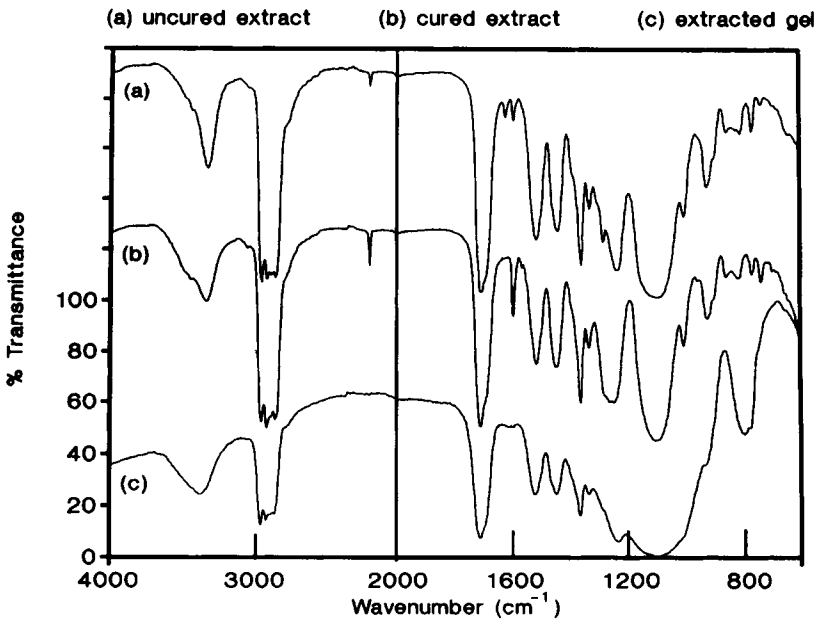

Figure 1 IR spectra of (a) the extract of uncured GNLB, (b) the extract from cured GNLB, and (c) the extracted GNLB gel (multiple internal reflectance).

tained in $CDCl_3$ with a model EM 690 Varian spectrometer. The extract from the uncured material exhibited seven main absorption regions that were interpreted in terms of the reaction product of hydroxyethyl methacrylate (HEMA) and α,ω-di-isocyanato-terminated polypropylene oxide. The δ values and assignments were 0.9–1.8 (doublet from the CH_3 in the propylene oxide units), 2.0 (singlet from the CH_3 of methacrylate), 3.3–4.0 (multiplet from the CH and doublet from the CH_2 of propylene oxide), 4.0–4.5 (singlet from the CH_2 of the ethylene oxide unit in HEMA and multiplet from the CH_2 of the propylene oxide units next to urethane linkages), 4.7–5.1 (broad resonance due to the exchangeable proton on the urethane linkage), 5.5–6.2 (doublet due to the HEMA olefinic protons), and 7.3–7.9 (multiplet from aromatic protons in the plasticizer). The NMR spectrum of the extract from the cured GNLB material did not exhibit the methyl, methylene, or olefinic resonance associated with HEMA. All the other peaks were present in the spectrum; however, the aromatic multiplet was much stronger in comparison to the other peaks. This suggests that in addition to an aromatic species the paste contains a polyether urethane oligomer.

Estimates of the molecular weight distribution of the GNLB extracts were obtained by use of a Waters HPLC with refractive index detection and employing microstyrogel columns (pore sizes ranging from 10 to 10^5 nm) and tetrahydrofuran as solvent. The extracts of the cured and uncured materials exhibited multimodal distributions with the two dominant peaks at 460 and 12,900 and at 640 and 13,600 g/mol, respectively. In the estimation of the average molecular weight of the extracts, the difference in hydrodynamic volume of the polystyrene molecular weight standards and the samples was ignored. Another potential error associated with the variable sensitivity of the detector to the chemical structure of the oligomer and plasticizer was also neglected. The apparent number average molecular weight was estimated to be 2300 g/mol for the uncured extract and 1300 g/mol for the extract from the cured material.

The dependence of the depth of cure on the irradiation conditions was studied using methods developed previously.[8] Uncured material was packed into aluminum cylindrical molds that were either 4 mm (for GNLB) or 10 mm (for GNHB) in diameter and from 10 to 30 mm deep. In all cases, the mold depth was selected to exceed the expected depth of cure by 5 mm so that the intensity of back-scattered radiation was approximately constant. The exit window was placed 2 mm above the opening of the cylindrical mold. A PET film over the top surface of the uncured material was used to exclude air during photocuring. After photocuring the material for a specified period at 23°C, the specimen was removed from the mold and the uncured material scraped off with a plastic spatula and the depth of the remaining

material (the depth of cure) measured. Replicate measurements revealed that the error in determining the depth of cure was ±0.1 mm.

The attenuation coefficient of the uncured material was measured with a series 634 Varian UV-vis spectrometer fitted with an integrating sphere. In this technique, all the transmitted radiation, including the forward-scattered component, is collected by the photodetector. Although the Kubelka–Munk method[9] for analyzing the optical transmission data of light-scattering materials is more accurate than is the simple Lambert law, the latter is an adequate description in the region 450–500 nm for GNLB and GNHB as is illustrated in Figure 2. After irradiation, the absorbance of the material in the vicinity of 470 nm was reduced by 10%, due to partial depletion of the camphor-quinone.

Isothermal kinetic studies of the polymerization were performed with a Perkin-Elmer DSC 7 differential scanning calorimeter and the Delta Isothermal software. Calibration of the DSC was carried out with indium, zinc, and azobenzene standards. To irradiate the sample inside the DSC cell and to minimize the effect of the high levels of thermal radiation generated by the photocuring source, a modified DSC cell closure was constructed. This closure consisted of a circular PMMA sheet with two holes located immediately above the DSC pans. The radiation from the photocuring source was directed into a sheathed, 7 mm diameter fiber-optic bundle that was bifurcated at the opposite end into two 5 mm diameter fiber-optic leads. The end fittings of these leads were then fitted into the holes in the PMMA cover so that the exit windows of each fiber-optic lead was located 4 mm above the base of the DSC pan. From measurements of the attenuation of the radiation in the bifurcated lead, the spectral irradiance at the base of the DSC pan was calculated to be 1.7×10^{-3} W/cm^2/nm at 470 nm. This intensity was reduced by up to 1000-fold by placing glass neutral density filters between the exit window of the photocuring source and the fiber-optic bundle. The use of dual pan illumination reduced the heating effect of the photocuring source by approximately 90% so that the thermal imbalance due to the source was about 3.5 mW (and less if neutral density filters were used). Correction for the influence of this imbalance on the measurements was made by repeating the isothermal DSC run (including the irradiation treatment) on the cured specimen and by subtracting these data from the first run.

DSC studies were performed under N_2 or air atmospheres. For the former, approximately 10 mg of material was spread over the base of the 6.5 mm diameter DSC pan that was then placed in the DSC cell. Approximately 120 min of N_2 flow (at 20 cc/min) was required to purge O_2 from the material and the cell, prior to the photopolymerization study. To stimulate the effect of dissolved O_2 on the photocuring process, a sample of the air-saturated material was weighed into the pan and a 5.5 mm diameter PET coverslip was pressed over the material

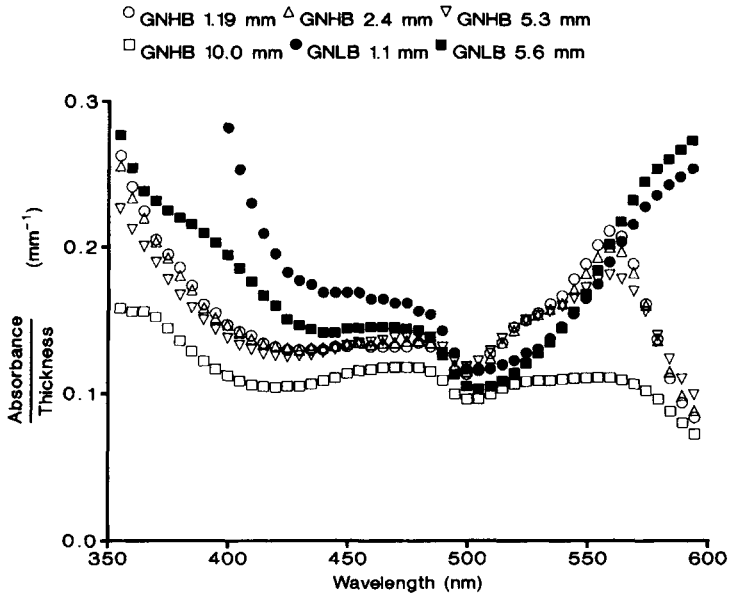

Figure 2 Attenuation coefficient for differing thicknesses vs. wavelength for GNLB (filled symbols) and GNHB (open symbols) at 23°C.

to minimize the diffusion of atmospheric oxygen into the film during the polymerization. Air was then passed over the pan during the thermal stabilizing period and photocuring run. In both cases, the sample thickness was less than 0.4 mm.

Studies of the shear modulus variation with irradiation time were performed in coaxial cylinder geometry as discussed in detail elsewhere.[10] The uncured material was contained in the annulus between an outer cylindrical mold and an inner rod, producing a tube of material 20 mm long and 3 mm thick with an outer diameter of 12.5 mm. The contact surfaces of both the outer cylindrical mold (fabricated from clear PMMA to allow irradiation of the material) and the inner rod were slightly grooved to maximize adherence of the material to the walls during deformation. The outer cylindrical mold was fastened to the base of a tensile-testing machine, and the inner rod was connected via the load cell to the crosshead. The crosshead was driven in a cyclic square wave fashion with a period of 20 s, and the force monitored as a function of time. Photopolymerization of the material was effected by irradiation through the outer mold using two photocuring sources. The stress relaxation modulus was calculated from the force at the end of each 10 s deformation phase.[10] Long-term stress relaxation experiments on fully cured cylindrical specimens were also performed in compression at a deformation ratio of 0.75, as described elsewhere.[11] Tear-energy measurements were performed on fully cured specimens using the trouser leg technique as described elsewhere.[12,13]

RESULTS AND DISCUSSION

Depth Effects

Since the GNLB and GNHB materials are intended for use in thick section, the depth of cure and its dependence on radiation conditions is important to their practical application. As noted above, when the material is photocured from the top surface, an elastomer is formed down to a specific depth known as the depth of cure. Below this depth, the material remains as a unpolymerized viscous liquid. Previous studies[8,14] of the photopolymerization of glass-forming dimethacrylate resins showed similar behavior. The occurrence of a specific depth of cure, below which no polymerization has commenced, can be explained[6,8] in terms of the attenuation of the radiation with depth and the consumption of free radicals by inhibitor species. Before irradiation commences, the concentration of inhibitor species (including O_2) is uniformly distributed throughout the material. On irradiation, initiator radicals are formed, leading to the production of chain radicals. However, inhibitor species compete with polymer chain growth and inhibit polymerization until virtually all of the inhibitor is consumed. Thus, under the particular radiation conditions, there exists a depth above which the inhibitor is depleted and where polymerization has occurred and below which the polymerization is totally inhibited. For monochromatic radiation, the rate of initiation at a depth l is given by[6,8]

$$R_i = \Phi R_{abs} = 2.303\Phi\epsilon_s[S]I_0 10^{-\epsilon l} \quad (1)$$

where R_i and R_{abs} are the rate of initiation and the rate of radiation absorption, I_0 is the incident radiation intensity at the surface, and $[S]$, Φ, and ϵ_s are the concentration, quantum yield, and decadic absorption coefficient of the photoinitiator, respectively. The term ϵ is the decadic attenuation coefficient of the material. Since $R_i t$ gives the concentration of radicals that are produced during an irradiation period (t), the local concentration of inhibitor, $[X]$, at a particular depth is related to the initial concentration, $[X]_0$, by[15]

$$[X] \approx [X]_0 - R_i t \quad (2)$$

provided that, on average, one chain is stopped by each inhibitor molecule. If each inhibitor consumed more than one radical, then eq. (2) could be modified for this effect. According to the scheme outlined above, the depth of cure occurs at the depth (D_c) at which the local concentration of inhibitor is depleted ($[X] \approx 0$), so that from eq. (2) we have

$$R_i \approx [X]_0/t \quad (3)$$

Thus, from eqs. (1) and (3), the depth of cure is

$$D = (1/\epsilon)\log(2.303\Phi\epsilon_s[S]I_0 t/[X]_0) \quad (4)$$

Since the depth of cure refers to a stage where few photons have been absorbed, $[S]$ can be approximated by the initial photoinitiator concentration.

If the radiation is polychromatic, then a more general integral form of eq. 4 should be used[6]; however, since the attenuation coefficient was found to be virtually independent of the wavelength between 450 and 500 nm (see Fig. 2), this integral form becomes equivalent to eq. (4).

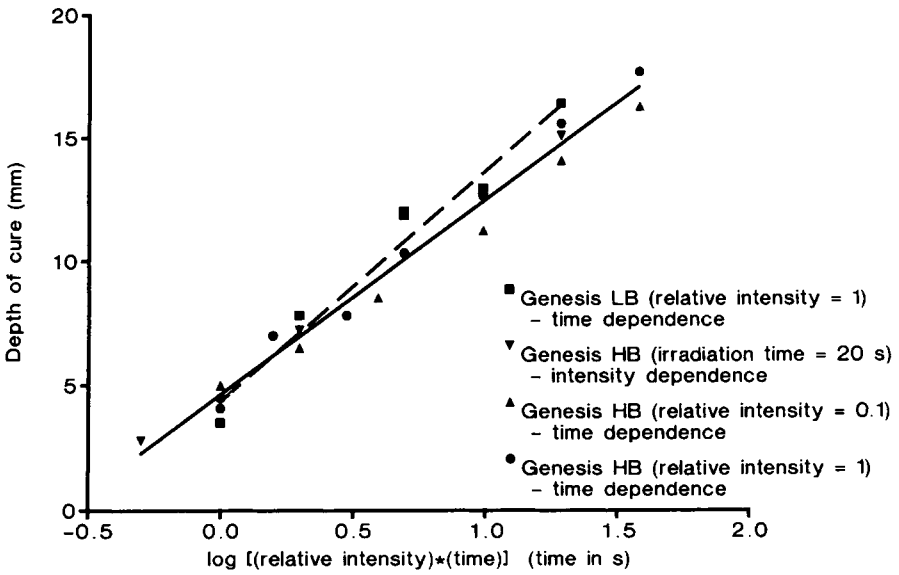

Figure 3 Dependence of the depth of cure on irradiation time and intensity for GNLB and GNHB at 23°C.

Figure 3 shows a plot of the depth of cure vs. the logarithm of I_0t according to eq. (4). The data for GNLB and GNHB are well fitted to the theory for variations in both irradiation time and intensity, as was found previously for glass-forming dimethacrylate systems.[8] The predicted attenuation coefficient given by the reciprocal of the slope for the fitted lines in Figure 3 are 0.11 and 0.13 mm^{-1} for GNLB and GNHB. These values agree well with the average attenuation coefficients of 0.113 ± 0.016 and 0.115 ± 0.008 mm^{-1}, respectively, obtained from least-square fits of the absorbance-thickness data in the region 450–500 nm. The near coincidence of the data in Figure 3 suggests [see eq. (4)] that the ratio of initiator to inhibitor in the two pastes is similar.

Photopolymerization in the Presence and Absence of Air

Figure 4 illustrates typical DSC traces for the photopolymerization. For a nonaccelerating reaction,

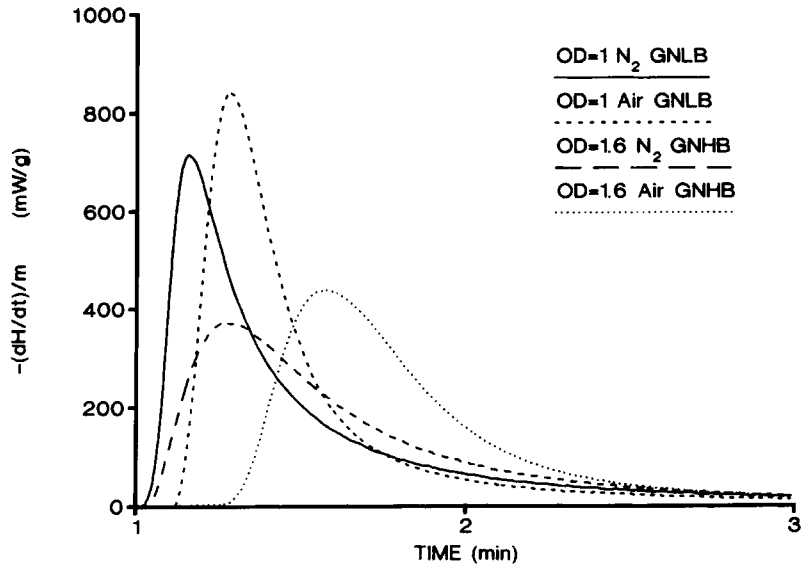

Figure 4 DSC curves of the photopolymerization of GNLB and GNHB under air and N_2 atmospheres at 30°C using neutral density filters with optical densities of 1.0 and 1.6. The photocuring source was triggered at the 1 min mark.

the DSC curve should show an abrupt rise in the DSC power signal (proportional to rate) at the start of the reaction, followed by a slow decline (exponential decline if the reaction is first order in monomer) as the monomer is consumed. Instead, the curves show a more or less gradual rise to a maximum occuring at approximately 20% conversion. This behavior has been noted by Tryson and Shultz[16] and has been interpreted as evidence of rate acceleration due to the gel effect.

The retarding effect of oxygen on the polymerization of GNLB and GNHB is also shown in the DSC traces of Figure 4. In the case where the samples were exposed to the N_2 atmosphere for 120 min, polymerization commences almost immediately on irradiation. In contrast, the air-saturated samples show an induction period prior to the commencement of polymerization. It appears likely that the inhibition is not solely due to the presence of O_2 but to an O_2-assisted phenolic inhibitor[17] since these inhibitor systems are commonly used as stabilizers[5] that are only active in the presence of O_2. The effect of the radiation intensity on the integrated DSC traces of GNLB in N_2 and air atmospheres is illustrated in Figure 5. As expected, an increase in the radiation intensity decreases the inhibition stage and increases the curing rate.

The thickness of the resin in the DSC experiments was less then 0.4 mm. For such thin films, eq. (1) can be simplified to

$$R_i = 2.303\Phi\epsilon_s[S]I_0 \qquad (5)$$

Thus, if polymerization is assumed[15] to be totally suppressed until all of the inhibitor is consumed, eqs. (3) and (5) show that the inhibition or onset time (t_{ons} as calculated by the DSC software) is related to the irradiation intensity by

$$t_{ons} = [X]_0/(2.303\Phi\epsilon_s[S]I_0) \qquad (6)$$

Figure 6 is a log-log plot of this relationship for GNLB and shows a slope of 0.90 ± 0.05 for the fitted line, which is in good agreement with the theoretical value of unity. In contrast, Fizet et al.[18] found a 0.75 power law for polymerization of trimethylolpropane triacrylate in solution, and in the bulk photopolymerization of epoxy–diacrylate oligomers, a 0.88 power-law relationship was observed.[19] In the latter study, the authors considered that the departure of this value from unity was significant and attributed the disagreement between theory and experiment to the consumption of more than one O_2 molecular per growing radical in the peroxidation process.

The simple expression for the rate of free-radical polymerization is[20]

$$-d[M]/dt = (k_p^2/k_t)^{1/2}R_i^{1/2}[M] \qquad (7)$$

where $[M]$ is the monomer concentration, k_p and k_t are the propagation and termination rate constants, and R_i is the rate of initiation. Substitution of eq. (5) into eq. (7) yields

$$-d[M]/dt = (k_p^2/k_t)^{1/2}(2.303\Phi\epsilon_s[S]I_0)^{1/2}[M] \qquad (8)$$

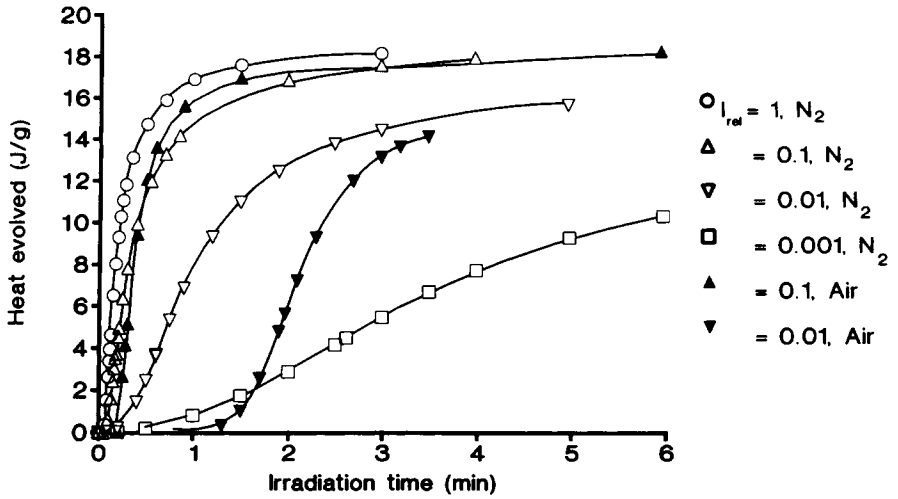

Figure 5 Heat evolved with time during the photopolymerization of GNLB under air (filled symbols) or N_2 (open symbols) atmosphere with varying radiation intensities at 30°C.

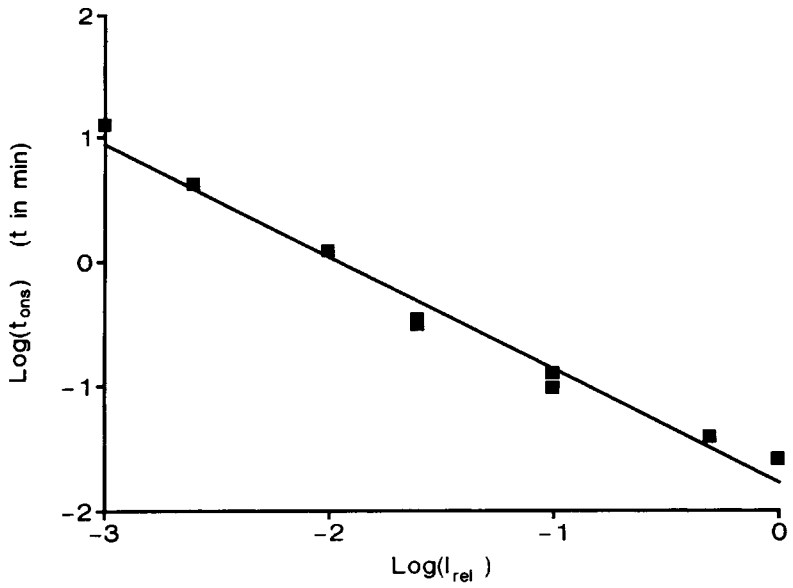

Figure 6 Log-log plot of onset (inhibition) time (t_{ons}) and relative radiation intensity (I_{rel}) during the photopolymerization of GNLB in an air atmosphere at 30°C.

Two parameters were used to measure the rate of polymerization. The reciprocal of the time taken to reach the maximum exotherm (occurring at about 20% conversion) is a direct measure of the polymerization rate if the shape of the DSC curve is unaffected by the radiation intensity. This was found to be a reasonable approximation in the present study. Since the time taken to reach the exotherm maximum (t_{pk} as calculated by the DSC software) includes the inhibition period, t_{ons} should be subtracted from t_{pk}. Figure 7 shows the log-log plot of the corrected time for maximum exotherm ($t_{pk} - t_{ons}$) and the relative radiation intensity for the polymerization of GNLB in a N_2 environment. The

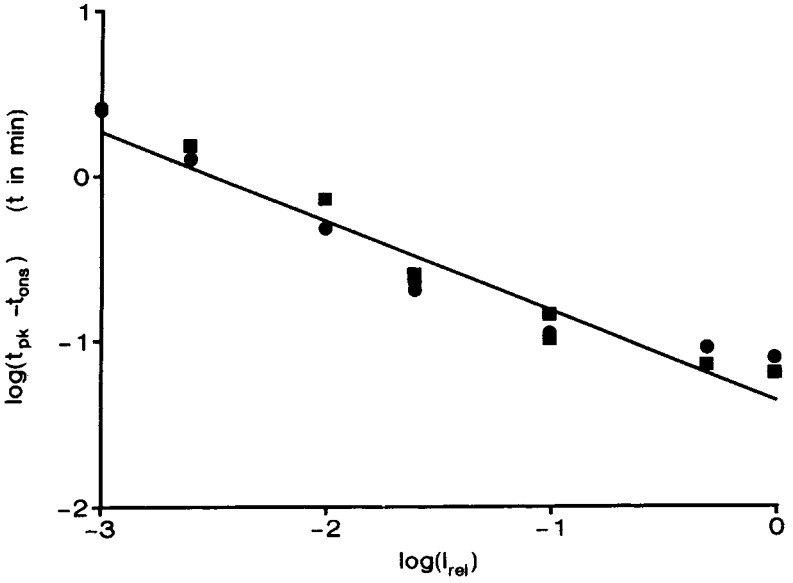

Figure 7 Log-log of $t_{pk} - t_{ons}$ (as a measure of the polymerization rate) vs. the relative radiation intensity (I_{rel}) during the photopolymerization of GNLB in a N_2 atmosphere (circles) and in air (squares) at 30°C. The term t_{ons} corrects for the inhibition caused by residual O_2 or inhibitors in the resin and was less than 25% of t_{pk} for the N_2 experiment.

related plot for the photocuring in an air environment is also given in Figure 7. The fitted slopes of these data were 0.54 ± 0.06 in each case. The second measure of the rate[21] was determined from the normalized maximum heat flow (dH/dt at the peak, divided by the sample mass). In this case, the intensity exponent was found to be 0.52 ± 0.04 and 0.55 ± 0.07 for N_2 and air environments, respectively. These values agree well with the theoretical value of 0.5 [eq. (8)] and the findings of Fizet et al.[18] for the solution polymerization of trimethylolpropane triacrylate. Parthasarathy et al.[22] also found that an intensity exponent of 0.5 for the aqueous polymerization of *N,N*-methylene bisacrylamide. Hayden and Mellville[23] have studied the intensity dependence of the rate for a 22 mol % solution of ethylene glycol dimethacrylate in methyl methacrylate. In this work, an exponent of 0.55–0.6 was found in the early stages of the polymerization; however, higher values were obtained in the regime of diffusion-controlled propagation. In contrast, for bulk photopolymerization of a mixture of diacrylates, Decker and Bendaikha[24] found an intensity order of 0.85 and Kloosterboer and Litjen[25] found an exponent of 0.7 for hexane diol diacrylate. In partial agreement with this finding, Tryson and Shultz[16] found that for hexane diol diacrylate the exponent ranged from 0.65 to 0.97 as the conversion increased from 15 to 54%. However, for pentaerythritol tetra-acrylate,[16] the value was 0.65 ± 0.05 for conversions ranging from 5 to 20%. One explanation for an intensity exponent greater than 0.5 is that the termination reaction tends toward a pseudo-first-order process, due to the presence of trace impurities that are relatively inefficient inhibitors but that terminate the growing radical chain.[16,24] Such behavior might be expected to occur for very reactive radicals (such as the acrylate radical[26]) or when the mobility of the growing radical is severely hindered by the developing network structure. However, for less reactive radicals (such as methacrylate radicals) in a less constrained environment (such as solution or with flexible dimethacrylate units), normal termination would be more likely and an intensity exponent of 0.5 would be found.

Figures 8 and 9 show the superposition of the DSC curves obtained by multiplying the polymerization time ($t_{pk} - t_{ons}$) by the root of the relative radiation intensity in accordance with eq. (8). Considering the range of intensities investigated and the small timescales involved in many of the scans, the data show reasonable overlap. Similar agreement is seen in Figure 10 for the DSC data of GNLB photocured in the presence of air.

Attempts at fitting the whole polymerization regime in Figures 8 and 10 to eq. (8) resulted in poor agreement. However, as noted above, the concentration of camphor-quinone is depleted during irradiation and the term $[S]$ in eq. 8 varies with time. Correction for this "dead-end polymerization" effect[27] for photopolymerization yields

$$-d[M]/dt = (k_p^2/k_t)^{1/2}(2.303\Phi\epsilon_s[S]_0 I_0)^{1/2} \times \exp(-\Phi I_0 \epsilon_s t/2)[M] \quad (9)$$

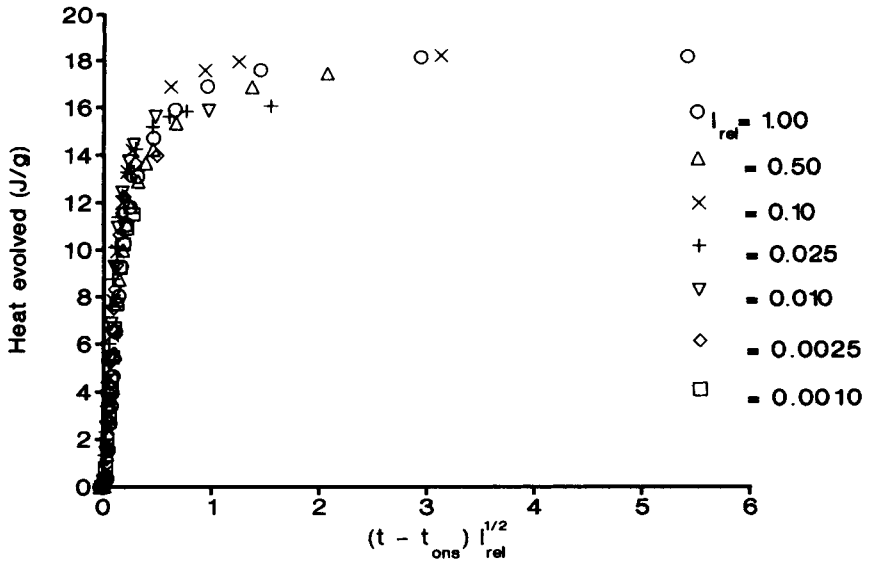

Figure 8 Heat evolved vs. $(t - t_{ons})I_{rel}^{1/2}$ during the photopolymerization of GNLB under a N_2 atmosphere with varying radiation intensities at 30°C.

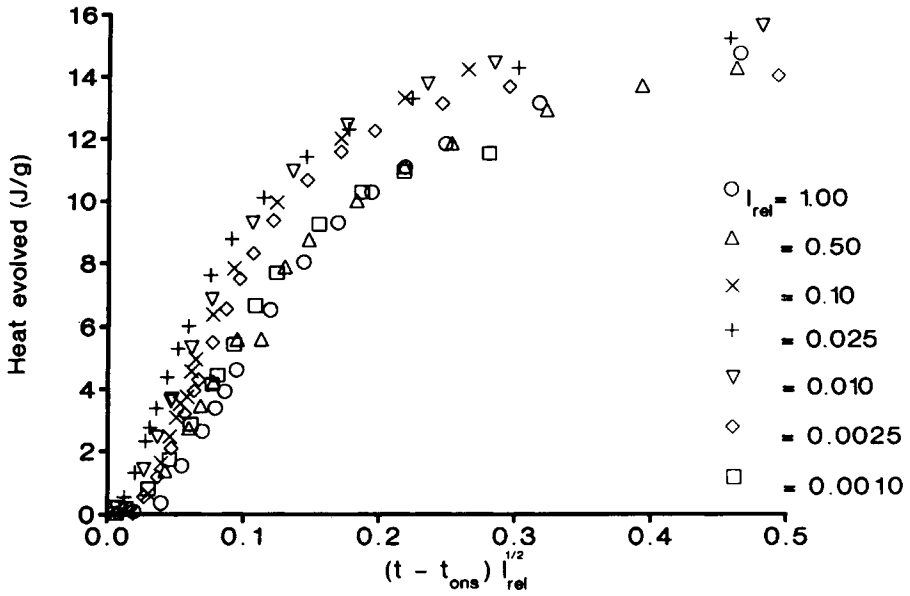

Figure 9 Heat evolved vs. $(t - t_{ons})I_{rel}^{1/2}$ during the photopolymerization of GNLB under a N_2 atmosphere at 30°C showing the early polymerization stages (see Fig. 8).

which can be integrated to give an expression for the conversion in terms of a double exponential expression. Curve fitting of the integrated DSC data to this equation resulted in good agreement; however, the two adjustable parameters in the fit [associated with the terms $(k_p^2/k_t)^{1/2}(2.303\Phi\epsilon_s \times [S]_0 I_0)^{1/2}$ and $\Phi I_0 \epsilon t/2$] did not depend on I_0 with the power predicted. Therefore, the high level of fit was considered to be partly fortuitous due to the inclusion of another adjustable parameter in the fitting procedure.

Given that free radical termination is diffusion controlled from the start of the polymerization and that k_t may vary be several orders of magnitude[23] as the reaction proceeds, it may appear that the form of eqs. (8) and (9) are totally inappropriate for in-

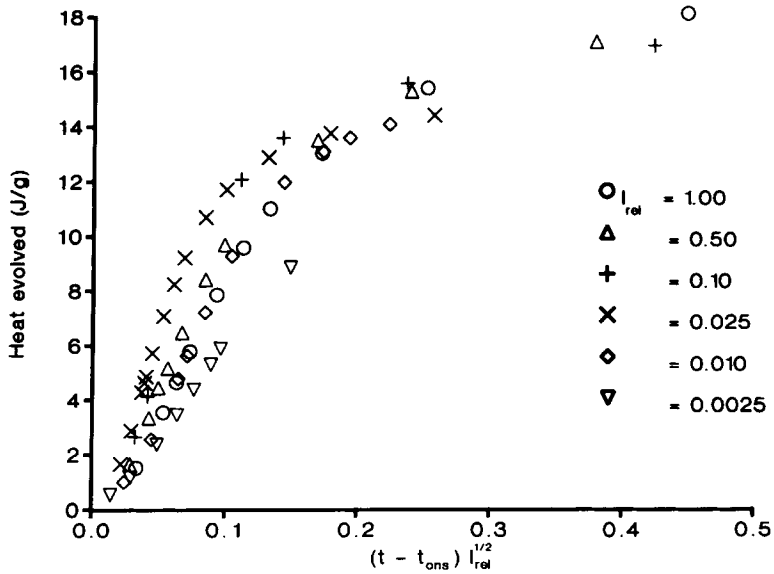

Figure 10 Heat evolved vs. $(t - t_{ons})I_{rel}^{1/2}$ during the photopolymerization of GNLB under an air atmosphere at 30°C showing the early polymerization stages.

terpreting the experimental data. For linear polymerization, the termination reaction is generally considered[28,29] to pass through the stages of segmental diffusion control (k_t independent of molecular weight), translational diffusion control (k_t dependent on chain radical size), and termination by propagation of the radical end (known[30] as "reaction diffusion"). The Trommsdorff effect, associated with chain entanglement of the growing radicals, occurs at the start of the translational diffusion region[28,31] and ends with the onset of reaction diffusion.[30,32] At high conversions, even the propagation reaction may be diffusion controlled due to the reduction in monomer mobility as vitrification is approached.[30,32]

For network-forming systems, it would appear that due to the rapid increase in viscosity the first segmental diffusion stage would end at very low conversions, after which translation diffusion would dominate. However, once a gel has formed, translational diffusion can only occur for radicals not attached to the gel.[33] Thus, termination by translational diffusion, which results in an acceleration of the rate (the Trommsdorff effect), should only be operative up to conversions slightly past the gel point because the probability that a propagating chain acquires a cross link during its life is quite high. For the remainder of the polymerization, termination should proceed by propagation of the chain ends (reaction diffusion). According to the analysis of Soh and Sundberg,[31] k_t under reaction diffusion control is primarily dependent on the term $k_p[M]$ provided that the entanglement spacing is considered to be constant. In the polymerization of di- or multifunctional vinyl monomers, diffusion control of propagation may occur well before vitrification. This is likely if the vinyl groups are separated by a semirigid spacer unit that reduces the mobility and thus the reactivity of the pendant vinyl groups.[1,34] However, if the vinyl groups are attached to flexible chains, as is the case for the present dimethacrylate resins, then the propagation reaction would be under chemical control throughout the whole conversion range. These considerations lead to a prediction that while the monomer exponent in eq. (8) may deviate from unity during the reaction the half-order dependence of the rate on intensity would remain.

The heats of polymerization (20 ± 2 J/g) for GNLB and GNHB were approximately equal, presumably because the resin content (40.2 and 37.4%, see Table I) does not vary significantly. The accuracy of the heat of polymerization is limited by the reduced rate in the latter stages of the reaction and the short duration (less than 10 min) of the photocuring runs. Based on the heat of polymerization of methyl methacrylate (578 J/g Ref. 35), and assuming 100% conversion (see Fig. 1), the molecular weight of the dimethacrylate was calculated to be approximately 2300 g/mol. This value is comparable to the values of 1680 ± 500 and 1942 ± 270 g/mol determined by IR spectroscopy (see Table I) for GNLB and GNHB, respectively.

Mechanical Properties

Whereas the DSC studies show that the photopolymerization is extremely fast, the dental application of the material also requires that the physical properties are also rapidly developed. Evidence for the fast buildup of properties is given in Figure 11 where the variation in the shear modulus with curing time is given. For comparison, the modulus cure profiles previously obtained[10] for two other dental elastomeric impression materials are shown. The first of these materials is a vinyl siloxane system (Permagum, manufactured by Espe, Germany) that consists[36] of a base paste containing a mixture of poly(methyl hydrogen siloxane) and α,ω-divinylpoly(dimethyl siloxane), and an accelerator paste containing the divinyl siloxane, poly(dimethyl siloxane), and a Pt salt catalyst. Network formation occurs by addition of the hydrosilane across the double bond. The other elastomeric material is an α,ω-di-imine-polyether (Impregum also manufactured by Espe) that is cationically polymerized with an alkyl-toluene sulphonate.[36] Despite the low radiation intensity utilized for the photocuring experiments (ca. 5×10^{-4} W/cm^2/nm at 470 nm), both GNLB and GNHB attain 90% of their final modulus in less than 5 min. This setting time is comparable to the vinyl siloxane elastomeric impression material and is much shorter than that of the imine-terminated polyether system. These conclusions also apply to other brands of the elastomeric impression materials.[10]

The stress-relaxation data for fully cured GNLB and GNHB are shown in Figure 12 and are compared with data previously obtained[11] for an imine-terminated polyether (Impregum), a vinyl siloxane (Permagum light body), and a PbO_2-cured polysulphide (Ultralastic light body, manufactured by SDI, Australia). The rate of stress relaxation in the polysulphide network is reasonably fast due to the disulphide bond-interchange process.[11] Of the other systems shown in Figure 12, the rate of stress relaxation for the dimethacrylate networks is the most rapid, suggesting[37] that their structure is imperfect and contains temporary entanglements that relax

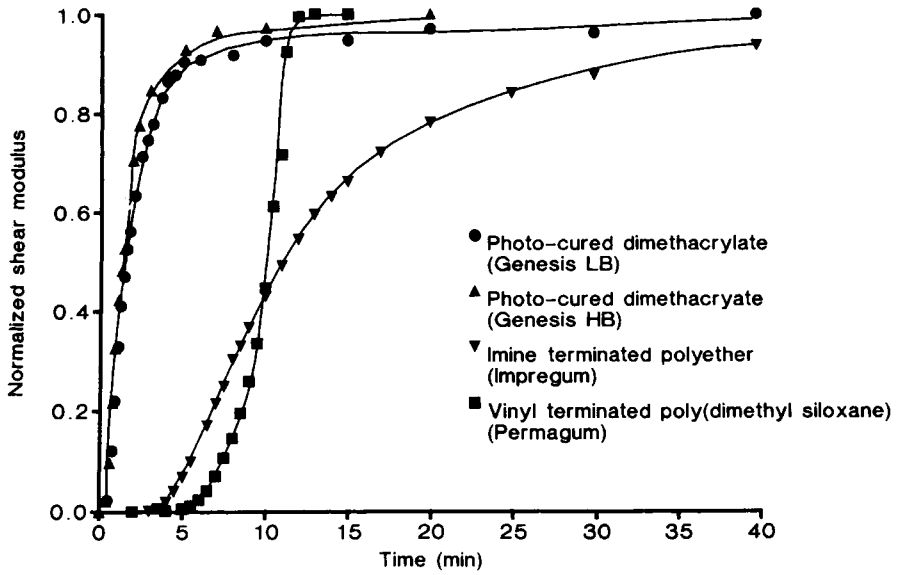

Figure 11 Dependence of the shear modulus on irradiation time for GNLB and GNHB. The radiation intensity at 470 nm was 5.4×10^{-4} W/cm^2/nm. For comparison, the modulus data for the two component vinyl-terminated poly(dimethyl siloxane) and di-imine-terminated polyether elastomers are shown. The curing temperature was 23°C.

through a reptation process. It is interesting to speculate that the high level of stress relaxation observed in the polysulphide and dimethacrylate networks may provide mechanisms of energy dissipation during tear,[38] resulting in the higher tear energies shown in Table II.

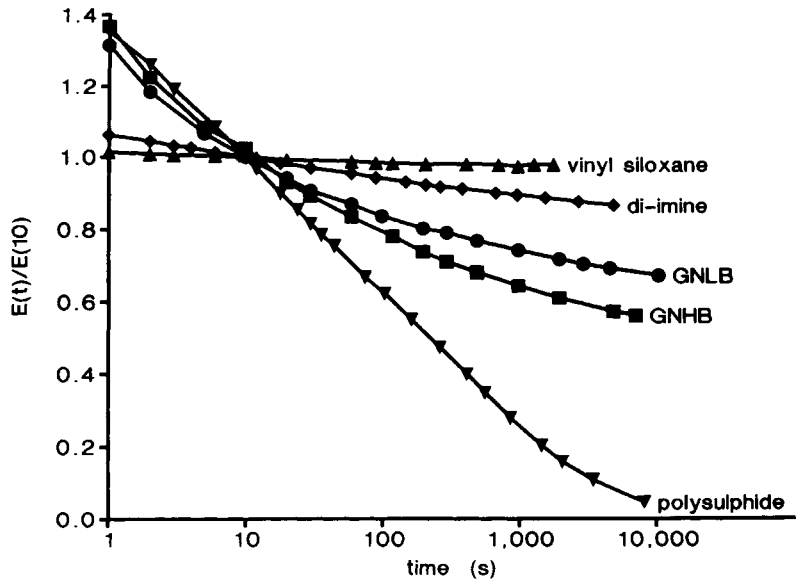

Figure 12 Relative stress relaxation modulus (at 23°C) in compression, $E(t)/E(10)$, as a function of relaxation time (t in s) for GNLB [$E(10)$ = 2.5 MPa], GNHB [$E(10)$ = 7.9 MPa], imine terminated polyether [$E(10)$ = 3.6 MPa], vinyl-terminated polysiloxane [$E(10)$ = 2.25 MPa] and polysulphide [$E(10)$ = 0.8 MPa] elastomers. The stress relaxation experiments commenced between 20 and 30 min after the start of polymerization.

Table II Comparison of Tear Energies for GNLB and GNHB with Other Elastomers

Material Type	Trade Name	Wt % Filler[a]	Tear Energy[b] (N mm)
Hydroxy-terminated polysiloxane	Xantopren plus	18	0.46 ± 0.01
Vinyl-terminated polysiloxane	Permagum (light)	45	0.45 ± 0.03
Imine-terminated polyether	Impregum	20	0.79 ± 0.04
Polyether urethane dimethacrylate	Genesis (light)—GNLB	40	1.1 ± 0.1
Polyether urethane dimethacrylate	Genesis (heavy)—GNHB	50	1.2 ± 0.1
PbO_2-cured polysulphide	Permalastic (light body)	41	3.0 ± 0.9

[a] From Ref. 36.
[b] From Ref. 12.

The equilibrium modulus (E_∞) for GNLB and GNHB was estimated from the stress relaxation data to be 1.7 and 3.9 MPa, respectively. The modulus of a filled elastomer can be related to the concentration (ν) of elastically active strands by the expression[39,40]

$$E_\infty = 3[(f-2)/f]\nu RT\left[1 + \frac{1.25\phi}{1-\phi/\phi_m}\right]^2 \quad (10)$$

where ϕ and ϕ_m are the volume fraction of filler and maximum packing fraction (0.8 approx.), f is the functionality of the junction, T is the temperature, and R is the gas constant. Although only the polyether chain between the methacrylate units can be considered as Gaussian-like (as required by the theory of rubber elasticity), this error is ignored and the junction is identified as the reacted methacrylate unit when it is connected in three directions (f is 3) to the rest of the network. Assuming the density of the matrix and filler to be 1.0 and 2.5 g/cm^3, eq. (10) yields 5700 and 3500 g/mol for the molecular weight of the dimethacrylates in GNLB and GNHB. Since the networks may contain a considerable fraction of wasted (elastically inactive) loops such as primary cycles (formed through the reaction of a radical end with its pendant vinyl group[34]) and secondary cycles (created by the propagation of a chain through two pendant vinyl groups attached to a second chain[34]), these values should be greater than the range of 1680–2300 g/mol calculated from the DSC and IR data.

The author is grateful to Dr. Ezio Rizzardo and Mr. Bill Chong, CSIRO Division of Chemicals and Polymers, for performing the NMR and HPLC experiments and for assistance in their interpretation.

REFERENCES

1. J. G. Kloosterboer, *Adv. Polym. Sci.*, **84**, 1 (1988).
2. G. E. Green, B. P. Stark, and S. A. Zahir, *J. Macromol. Sci. Rev. Macro. Chem.*, **C21**, 187 (1981–82).
3. P. Hall, *Link*, **7**, 16 (1989).
4. W. D. Cook, D. R. Beech, and M. J. Tyas, *Biomaterials*, **6**, 362 (1985).
5. I. E. Ruyter and H. Oysaed, *Biocompatibility of Dental Materials*, D. C. Smith and D. R. Williams, Eds., C. R. C. Press, Boca Raton, FL, 1982, Vol. IV.
6. W. D. Cook, *Biomaterials*, **7**, 449 (1986).
7. H. Shintani, T. Inoue, and M. Yamaki, *Dent. Mat.*, **1**, 123 (1985).
8. W. D. Cook, *J. Macromol. Sci. Chem.*, **A17**, 99 (1982).
9. P. Kuebelka, *J. Opt. Soc. Am.*, **38**, 448 (1948).
10. W. D. Cook, *J. Biomed. Mater. Res.*, **16**, 345 (1982).
11. W. D. Cook, *J. Biomed. Mater. Res.*, **15**, 449 (1981).
12. W. D. Cook, F. Liem, P. Russo, M. Scheiner, G. Simkiss, and P. Woodruff, *Biomaterials*, **5**, 275 (1984).
13. A. G. Rivlin, *J. Appl. Polym. Sci.*, **3**, 168 (1960).
14. I. E. Ruyter and H. Oysaed, *Acta. Odontol. Scand.*, **40**, 179 (1982).
15. G. M. Burnett, High Polymers, Interscience, New York, 1954, Vol. III, p. 110.
16. G. R. Tryson and A. R. Shultz, *J. Polym. Sci. Polym.*, **17**, 2059 (1979).
17. R. G. Caldwell and J. L. Ihrig, *J. Am. Chem. Soc.*, **84**, 2878 (1962).
18. M. Fizet, C. Decker, and J. Faure, *Eur. Polym. J.*, **21**, 427 (1985).
19. C. Decker and A. D. Jenkins, *Macromolecules*, **18**, 1241 (1985).
20. P. J. Flory, *Principles of Polymer Chemistry*, Cornell University Press, Ithaca, NY, 1953, Chap. 4.
21. J. E. Moore, S. H. Schroeter, A. R. Shultz, and L. D. Stang, Am. Chem. Soc. Symp. Ser. 25, American Chemical Society, Washington, DC, 1976, p. 90.
22. T. Parthasarathy, K. Nageswar Rao, B. Sethuram, and T. Navaneeth Rao, *J. Macromol. Sci. Chem.*, **A26**, 1355 (1989).

23. P. Hayden and H. Mellville, *J. Polym. Sci.*, **43,** 215 (1960).
24. C. Decker and T. Bendaikha, *Eur. Polym. J.*, **20,** 753 (1984).
25. J. G. Kloosterboer and G. F. C. M. Lijten, *Polym. Commun.*, **28,** 2 (1987).
26. R. W. Lenz, *Organic Chemistry of Synthetic High Polymers*, Interscience, New York, 1967, p. 335.
27. A. V. Tobolsky, *J. Am. Chem. Soc.*, **80,** 5927 (1958).
28. S. K. Soh and D. C. Sundberg, *J. Polym. Sci. Polym. Chem. Ed.*, **20,** 1299 (1982).
29. J. M. Dionisio and K. F. O'Driscoll, *J. Polym. Sci. Polym. Chem. Ed.*, **18,** 241 (1980).
30. M. Stickler, *Makromol. Chem.*, **184,** 2563 (1983).
31. S. K. Soh and D. C. Sundberg, *J. Polym. Sci. Polym. Chem. Ed.*, **20,** 1315 (1982).
32. S. K. Soh and D. C. Sundberg, *J. Polym. Sci. Polym. Chem. Ed.*, **20,** 1331 (1982).
33. M. Gordon and R.-J. Roe, *J. Polym. Sci.*, **21,** 57 (1956).
34. D. T. Landin and C. W. Macosko, *Macromolecules*, **21,** 846 (1988).
35. H. Sawada, *J. Macromol. Sci.*, **C3,** 313 (1969).
36. W. D. Cook, *J. Biomed. Mater. Res.*, **16,** 315 (1982).
37. J. D. Ferry, *Viscoelastic Properties of Polymers*, 2nd ed., Wiley, 1970, Chap. 14.
38. A. Ahagon and A. N. Gent, *J. Polym. Sci.*, **13,** 1903 (1975).
39. J. D. Ferry, *Viscoelastic Properties of Polymers*, 2nd ed., Wiley, New York, 1970, p. 456.
40. W. W. Graessley, *Macromolecules*, **8,** 865 (1975).

Received April 23, 1990
Accepted June 18, 1990